Self-Reconfiguration Using Graph Grammars for Modular Robotics

Daniel Pickem * **Magnus Egerstedt** **

* *Georgia Institute of Technology, Atlanta, GA 30332 USA (e-mail: daniel.pickem@gatech.edu).*
** *Georgia Institute of Technology, Atlanta, GA 30332 USA (e-mail: magnus.egerstedt@gatech.edu)*

Abstract: In this paper, we apply graph grammars to self-reconfigurable modular robots and present a method to reconfigure arbitrary initial configurations into prespecified target configurations thus connecting the motions of modules to formal assembly rules. We present an approach for centralized reconfiguration planning and decentralized, rule-based reconfiguration execution for three-dimensional modular structures. The reconfiguration is done in two stages. In the first stage, paths are planned for each module and then rewritten into production rules as defined for graph grammars. Global knowledge about the configuration is available to the planner. In stage two, these rules are applied in a decentralized fashion by each node individually and with local knowledge only. We show that our approach yields a unique reconfiguration sequence and a graph grammar that results in the target configuration being the only reachable stable configuration.

1. INTRODUCTION

Modular robotics is the assembly of simple individual modules into a larger, functional robot. The benefit of constructing such modular robots out of smaller building blocks is that they can be rearranged into different configurations that can perform different functions and have different capabilities. In fact, the key advantages of modular robots are their potential for versatility, robustness, and low cost. The ability to reconfigure allows modular robots to adapt to new tasks and environments by changing their morphology. Broken modules can be replaced by functional ones or new modules can be added without changing the general functionality of the structure (see for example Yim et al. [2007]).

The goal of this work is to present a novel approach for the automatic reconfiguration of three-dimensional modular robots from an arbitrary initial configuration into a desired target configuration. This process is completed in two stages; the planning and the execution stage. In stage one, paths are planned for every module from its initial position to its target position. This planning is done in a centralized fashion with global knowledge. The resulting paths are then rewritten into a ruleset composed of production rules. This paper follows the general route laid down in Jones and Mataric [2003], where rules are automatically generated for two-dimensional structures. Three-dimensional structures were addressed in Brandt and Ostergaard [2004], albeit only for a much smaller class of systems compared to what is done in this paper.

For the algorithm presented in this paper, the initial configuration has to be known (as is also the case for Jones and Mataric [2003] and Brandt and Ostergaard [2004]). The dependence on initial configurations has been treated in Fitch et al. [2003] for manually defined rulesets. Other work on manually defined rulesets includes Butler et al. [2004] who have demonstrated the feasibility and scalability of rule-based self-reconfiguration. The rulesets in these papers do not contain graph grammatical production rules. Klavins [2007], on the other hand, manually synthesizes graph grammars for two-dimensional reconfiguration and we will follow the approach for three-dimensional structures in this paper.

The main contribution of this paper is the automatic generation of graph grammars for the self-reconfiguration of three-dimensional structures. Any arbitrary initially connected configuration composed of cubic modules can be reconfigured into any prespecified target configuration. The only constraints of our method are that both configurations are not allowed to contain any enclosures and have to feature an overlapping region that contains at least one module. Our approach yields a unique reconfiguration sequence and we prove that the target configuration is the only possible outcome of the reconfiguration sequence.

The rest of this paper is organized as follows: Section 2 presents previously done work in the field of self-reconfiguration. Section 3 describes our system representation and introduces the notation used in this paper. Section 4 explains the path planning approach used for the reconfiguration. Section 5 introduces graph grammar concepts and their application to self-reconfiguration and presents the main contribution of this paper. Section 6 presents our findings and Section 7 concludes this paper.

2. RELATED WORK

Much work has been done on the planning aspect of self-reconfiguration. Available planning strategies include hierarchical or layered planning, rule-based planning, and Markov decision process-based planning. This section specifically presents relevant rule-based reconfiguration approaches. Butler et al. [2004] describe a rule-based

system inspired by cellular automata. Their rulesets are designed manually and enable groups of modules to split and merge, climb over or move around obstacles, or move through tunnels. Brandt and Ostergaard [2004] introduce a rule-based control strategy for the ATRON system (see Brandt et al. [2007]). Their rules take connectivity information into account and are automatically generated. They introduce wild card rules to reduce the size of the ruleset. Jones and Mataric [2003] show rule-based control for two-dimensional structures. The rules are automatically generated and only use connectivity information to check for rule applicability. These rules are either manually synthesized, limited to a specific class of structures or do not guarantee a successful reconfiguration to the target structure.

Many other approaches have been presented in the literature. One example is the approach shown in Fitch and Butler [2007] who formulate the reconfiguration problem as a Markov decision process. According to the paper, a solution is obtained in sublinear time, albeit only for the purpose of locomotion of three-dimensional structures. Their algorithms can handle configurations containing up to 75^3 modules and map actions to lattice positions instead of to modules. Because an optimal action is associated with each lattice position, the same action is applied to each module at a certain position, which only works for homogeneous systems. Unlike Fitch and Butler [2007], our approach can handle arbitrary reconfigurations and includes locomotion as a special case.

Graph grammars, as a tool for manipulating graphs, have also been applied to modular robotics. Klavins [2007], for example, uses graph grammars to reconfigure programmable parts, a triangle shaped hardware implementation. He manually synthesizes rulesets that are designed to form specific structures out of the triangular modules. As opposed to our system, Klavins [2007] allows multiple rules to be applicable to the whole system at the same time. Unlike for our system, this approach does not guarantee a uniquely determined reconfiguration sequence or the reaching of the target configuration.

3. SYSTEM REPRESENTATION

In this paper we investigate a modular robotic system whose basic building blocks are visually represented by cubes (see Fig. 1). Moreover, no physical constraints beyond collision-avoidance such as gravity, module masses, or forces are taken into account. Additionally, the entire reconfiguration process happens in free space and is not restrained by walls, floors, or any other obstacles. These assumptions are made in order to focus the contribution on the self-reconfiguration process rather than on implementation-specific details.

Following the taxonomy in Yim et al. [2007], modular robots can generally be categorized into lattice-type and chain-type architectures. We present a lattice-based system that is embedded in a discrete coordinate system using the sliding cube model (see Fitch et al. [2003]). In the sliding cube model, every module (also referred to as node) is represented as a cube with dimension δ (w.l.o.g. we use unit cubes, i.e. $\delta = 1$), an origin $x_i \in \mathbb{Z}^3$, and a globally unique integer identifier. A cube features connectors on each surface and is capable of executing motions. A motion can be generally described as a function $f(x_i, m) = x_i + m$ where $x_i \in \mathbb{Z}^3$ and $m \in \mathbb{Z}^3$. Therefore, a motion moves a cube to a new position in $\mathbb{Z}^3$. In particular, the cubes in our system are capable of two primitive motions - sliding along a surface made of other cubes as well as convex transitions to orthogonal surfaces.

Definition 1. A *sliding motion* m_s is such that $f(x_i, m_s) = x_i + m_s$ where $x_i \in \mathbb{Z}^3$ and $m_s \in \mathbb{Z}^3 \wedge m_s \in \mathcal{M}_s$. $\mathcal{M}_s$ is the set of all possible sliding motions and is defined as $\mathcal{M}_s = \{m \in \mathbb{Z}^3 | m_x = 1 \vee m_y = 1 \vee m_z = 1 \wedge m_x + m_y + m_z = 1\}$.

An example of a sliding motion would be $f(x_i, m_s)$: $(x_{i,x}, x_{i,y}, x_{i,z}) \xrightarrow{m_s} (x_{i,x} + 1, x_{i,y}, x_{i,z})$, which moves a cube located at x_i in the positive direction on the x-axis.

Definition 2. A *convex motion* m_c is such that $f(x_i, m_c) = x_i + m_c$ where $x_i \in \mathbb{Z}^3$ and $m_c \in \mathbb{Z}^3 \wedge m_c \in \mathcal{M}_c$. $\mathcal{M}_c$ is the set of all possible convex motions and is defined as $\mathcal{M}_c = \{m \in \mathbb{Z}^3 | m_x < 2 \wedge m_y < 2 \wedge m_z < 2 \wedge m_x + m_y + m_z = 2\}$.

An example of a convex motion would be $f(x_i, m_c)$: $(x_{i,x}, x_{i,y}, x_{i,z}) \xrightarrow{m_c} (x_{i,x} + 1, x_{i,y} + 1, x_{i,z})$, which moves a cube located at x_i in the positive direction on the x-axis and the y-axis at the same time.

Note, however, that we will not allow the application of sliding or convex motions unless they are feasible. In fact, the movement of individual cubes requires a connected substrate of other cubes. Such a connected arrangement is referred to as a configuration, i.e. a configuration describes a geometric arrangement of cubes. The representable space of our system is $\mathbb{Z}^{3N}$ and any configuration $\mathcal{C}$ is a subset of the representable space, $\mathcal{C} \subset \mathbb{Z}^{3N}$.

One way in which a configuration can be described is through three adjacency matrices and a labelset. Every adjacency matrix describes the adjacency of cubes along one dimension. Its entries are given by $g(\mathcal{C}) = (A_k, l)$, where

$$A_k = [a_{i,j,k}] = \begin{cases} 1 & \text{if } (x_i - x_j)^T \cdot b_k = 1 \\ -1 & \text{if } (x_i - x_j)^T \cdot b_k = -1 \\ 0 & \text{otherwise} \end{cases}$$

$$l(i) = l(c_i), c_i \in \mathcal{C}, i, j \in \{1, \ldots, N\}$$

Here, k represents one dimension of the configuration space $\mathbb{Z}^{3N}$ spanned by the three orthogonal base vectors b_k, c_i stands for a cube of the configuration $\mathcal{C}$, and the labels $l(i)$ of node i are the same as the labels of cube c_i. One adjacency matrix for every dimension of the configuration space is required to encode the three-dimensional geometry of the configuration. The advantage of our adjacency representation is that we can encode the vertex set as well as the edge set of the represented graph in one data structure. Just the labels of each vertex have to be stored separately. An example of the adjacency representation is shown in Fig. 2(a) and Fig. 3. Alternatively, a configuration can be represented as a labeled graph:

Definition 3. The *represented graph* $G = (V, E, l_G)$ is composed of the vertex set V, the edge set E, and edge and vertex label set l_G and is derived from (A_k, l) via the adjacency-to-graph mapping $h(A_k, l) = (V, E, l_G)$. V is a finite set of integers corresponding to the cube IDs, i.e. $V = \{1, \ldots, N\}$, where N is the total number of cubes. E is

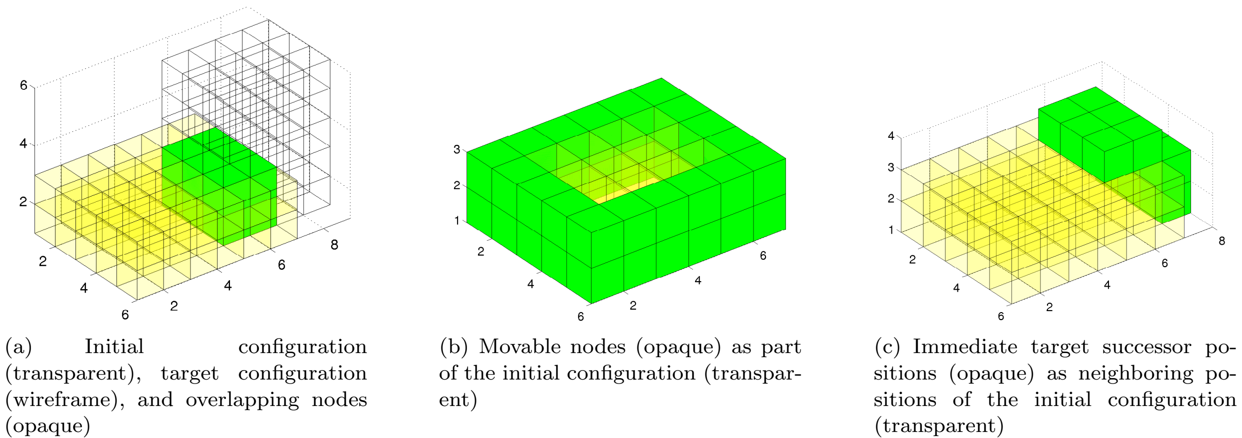

(a) Initial configuration (transparent), target configuration (wireframe), and overlapping nodes (opaque)

(b) Movable nodes (opaque) as part of the initial configuration (transparent)

(c) Immediate target successor positions (opaque) as neighboring positions of the initial configuration (transparent)

Fig. 1. Graphical representation of the overlapping, movable, and immediate target successor set in the simulator

derived from the three adjacency matrices A_k as $E \subseteq V \times V$, with $e_{i,j} \in E$ if $A_{i,j,k} \neq 0$ for some $k \in \{1, 2, 3\}$. l_G contains edge labels and vertex labels and is derived from A_k and l as follows:

$$l_G(v_i) = l(c_i) \qquad \text{with } v_i \in V, c_i \in \mathcal{C}$$
$$l_G(e_{i,j}) = sign(A_{i,j,k})b_k \qquad \text{with } e_{i,j} \in E \text{ and } A_{i,j,k} \neq 0$$

Here, $i, j \in \{1, \ldots, N\}$, $l(c_i) \in l$, and b_k is a base vector. The vertex labels of $v_i \in G$ are the same as the labels for the cubes $c_i \in \mathcal{C}$. A graphical representation of a graph G is shown in Fig. 2(b). G is a directed, labeled graph that preserves the three-dimensional structural information of the configuration.

The graph notation is required to define graph grammar rules and apply them to our system in Section 5.2. An advantage of the graph notation is that we can apply graph theoretical concepts such as the notion of connectivity. A reduced version of the represented graph G, the connectivity graph, is sufficient for the connectivity check.

Definition 4. The *connectivity graph* $G_c = (V, E, l_{G_c})$, where V and E are as before and the labels l_{G_c} are defined as follows: $l(v_i) = l(c_i)$ for $v_i \in V$ and $c_i \in \mathcal{C}$, i.e. the labels of nodes $v_i \in G_c$ are the same as the labels of cubes $c_i \in \mathcal{C}$. The connectivity graph does not contain any edge labels and stores connectivity information in only one adjacency matrix A, which is defined as

$$A_{i,j} = |sign(\sum_{k=1}^{3} |A_{i,j,k}|)| \quad i, j \in \{1, \ldots, N\}$$

In this paper, we assume that the initial configuration $\mathcal{C}^{\mathcal{I}}$ and the target configuration $\mathcal{C}^{\mathcal{T}}$ are known and contain the same number of modules. We employ a two-stage planning process. In stage one, our algorithm finds the overlapping region $\mathcal{O}$ of both $\mathcal{C}^{\mathcal{I}}$ and $\mathcal{C}^{\mathcal{T}}$ and then calculates a path for every node $c_i \in \mathcal{C}^{\mathcal{I}} \setminus \mathcal{O}$ to a position $c_j \in \mathcal{C}^{\mathcal{T}}$ (see Section 4). Furthermore, a ruleset or graph grammar is generated from these paths. In stage two, each node then executes rules that can be checked locally for applicability. Local in this context means that each rule describes a neighborhood of the current cube and can only manipulate cubes in that neighborhood. The rule execution is done in a decentralized way during which each cube can just access neighborhood information and the ruleset (see Section 5).

4. PATH PLANNING

The reconfiguration process requires us to move cubes from their initial positions to their target positions. Therefore, we have to calculate paths for cubes $c_i \in \mathcal{C}^{\mathcal{I}}$ to their desired positions in $c_j \in \mathcal{C}^{\mathcal{T}}$. Cubes c_i in the initially overlapping region $\mathcal{O}_{init} = \mathcal{C}^{\mathcal{I}} \cap \mathcal{C}^{\mathcal{T}}$ (see Fig. 1(a)), do not have to be moved and are excluded from the planning process. The planning stage is composed of multiple steps, which are the calculation of the currently overlapping region $\mathcal{O} = \mathcal{C} \cap \mathcal{C}^{\mathcal{T}}$, the movable set $\mathcal{M}$, the immediate target successor set $\mathcal{R}$, the node path calculation (for every cube $c_i \in \mathcal{C}^{\mathcal{I}} \setminus \mathcal{O}_{init}$), and the ruleset generation (see Section 5.2). In this section, we will formally define $\mathcal{M}$ and $\mathcal{R}$, the notion of articulation points and paths, and describe the planning approach.

Definition 5. An *articulation point* v in a graph G is a node whose removal would increase the number of connected components $c(G)$, i.e. $c(G - v) > c(G)$ [1]. In other words, the removal of v would disconnect the graph (see Fig. 2(c)).

A connected graph G has only one connected component, $c(G) = 1$. Our self-reconfigurable system has to remain connected at all times to guarantee a successful reconfiguration. In order to enforce this requirement, we have to ensure that a node that is an articulation point of the connectivity graph is never moved. The movable set is therefore defined as follows:

Definition 6. The *movable set* $\mathcal{M}$ is a set of cubes that can be moved without disconnecting the configuration and is defined as $\mathcal{M} = \{c_i \in \mathcal{C} | c_i \in \mathcal{C}^{\mathcal{I}} \setminus \mathcal{O} \wedge c_i \notin \mathcal{A}(\mathcal{C}) \wedge |\mathcal{N}_1(c_i, \mathcal{C})| \leq 5\}$. $\mathcal{N}_1(c_i, \mathcal{C})$ is the one-hop neighborhood and defined as $\mathcal{N}_1(c_i, \mathcal{C}) = \{c_j \in \mathcal{C} | dist(c_i, c_j) = 1\}$. $\mathcal{A}(\mathcal{C})$ is the set of articulation points of the graph representing the current configuration $\mathcal{C}$ (see Fig. 2(c)).

This definition is based on the sliding cube model (see Fitch et al. [2003]) and only allows modules on the surface

[1] Connected components of a graph G are its maximal connected subgraphs.

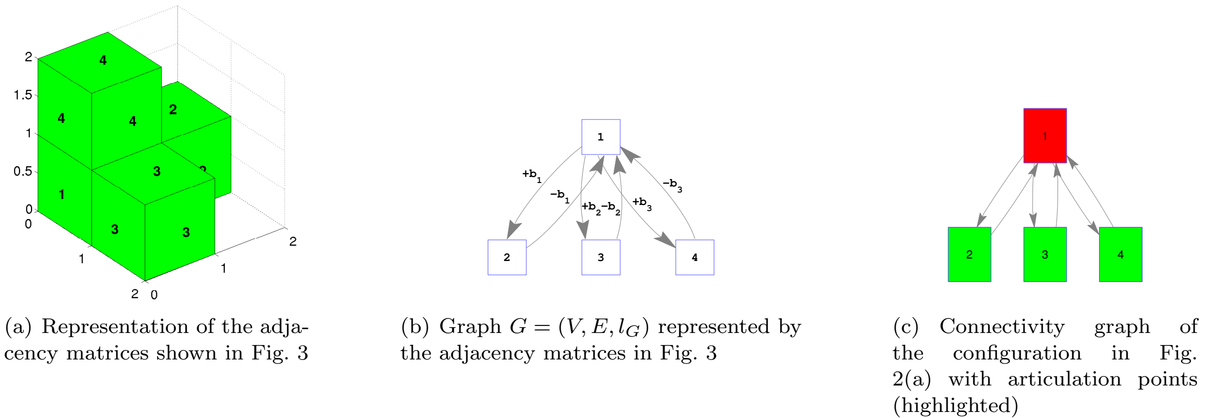

(a) Representation of the adjacency matrices shown in Fig. 3

(b) Graph $G = (V, E, l_G)$ represented by the adjacency matrices in Fig. 3

(c) Connectivity graph of the configuration in Fig. 2(a) with articulation points (highlighted)

Fig. 2. Graphical representation of the adjacency matrices in Fig. 3 and the corresponding graph.

$$A_1 = \begin{pmatrix} 0 & 1 & 0 & 0 \\ -1 & 0 & 0 & 0 \\ 0 & 0 & 0 & 0 \\ 0 & 0 & 0 & 0 \end{pmatrix} A_2 = \begin{pmatrix} 0 & 0 & 1 & 0 \\ 0 & 0 & 0 & 0 \\ -1 & 0 & 0 & 0 \\ 0 & 0 & 0 & 0 \end{pmatrix} A_3 = \begin{pmatrix} 0 & 0 & 0 & 1 \\ 0 & 0 & 0 & 0 \\ 0 & 0 & 0 & 0 \\ -1 & 0 & 0 & 0 \end{pmatrix}$$

Fig. 3. Adjacency matrices for the configuration in Fig. 2(a)

of the configuration to be relocated. This is because Def. 6 excludes immobile cubes within the configuration (i.e. cubes that have six neighbors) from the movable set. While $\mathcal{M}$ is a set of movable cubes, we need to find potential target positions for cubes $c_i \in \mathcal{M}$ - the immediate target successor set $\mathcal{R}$.

Definition 7. The *immediate target successor set* $\mathcal{R}$ is defined as positions $c_j \in \mathcal{C}^{\mathcal{T}}$ that are adjacent to the current configuration, i.e. lie in the one-hop neighborhood $\mathcal{N}_1(\mathcal{C})$ of the current configuration $\mathcal{C}$ as well as in the target configuration $\mathcal{C}^{\mathcal{T}}$. $\mathcal{R} = (\mathcal{C}^{\mathcal{T}} \cap \mathcal{N}_1(\mathcal{C})) \setminus \mathcal{C}$, where $\mathcal{N}_1(\mathcal{C}) = \{c_j | c_j \notin \mathcal{C} \wedge c_i \in \mathcal{C} \wedge dist(c_i, c_j) = 1\}$ (see Fig. 1(c)). Therefore, $\mathcal{R}$ is a subset of $\mathcal{N}_1(\mathcal{C})$.

Note that $\mathcal{N}_1(\mathcal{C})$ is the one-hop hull of the current configuration $\mathcal{C}$ and at the same time the planning space for the path planner. In that planning space, we plan a path p_i for a single cube at a time, i.e. from $c_i \in \mathcal{M}$ to $c_j \in \mathcal{R}$. We know by assumption that $\mathcal{R}$ is nonempty unless the target configuration has already been assembled. The path p_i is only allowed to contain positions $c_k \in \mathcal{N}_1(\mathcal{C})$ and use primitive motions to move the current cube c_i.

Definition 8. A path is a concatenation of motions $m \in \{m_c, m_s\}$ (see Def. 1 and Def. 2) that move cube $c_i \in (\mathcal{C}^{\mathcal{I}} \setminus \mathcal{O}) \cap \mathcal{M}$ to position $c_j \in \mathcal{C}^{\mathcal{T}} \cap \mathcal{R}$. The length of the path p_i, or the total number of motions, is denoted as $|p_i|$.

Both $\mathcal{M}$ and $\mathcal{R}$ define a set of cubes. Before we can plan a path for a cube c_i to a position c_j, we need to define an assignment. Therefore, we calculate the pairwise costs between any two cubes $c_i \in \mathcal{M}$ and $c_j \in \mathcal{R}$ and pick the pair of cubes with the lowest cost. The assignment resulting from this greedy approach is then used as input for the path planner. This process is repeated for all cubes $c_i \in \mathcal{C}^{\mathcal{I}} \setminus \mathcal{O}$ and paths are computed to their respective target positions $c_j \in \mathcal{C}^{\mathcal{T}}$. Note that this approach ensures that progress is never blocked and the target configuration will indeed be assembled if it is possible.

In this paper, we use A* for path planning together with the Manhattan distance as cost metric as it most accurately represents the discrete lattice structure of our system and the possible movements of the nodes. Other planners can of course be used, but we made this choice due to A*'s properties of optimality and completeness, which ensure us to find the optimal paths in polynomial time assuming that the heuristic meets the requirements defined in Russell and Norvig [2003]. The Manhattan distance we use as heuristic does fulfill these criteria. The result of the path planning stage is a set of paths that describe the complete reconfiguration from $\mathcal{C}^{\mathcal{I}}$ to $\mathcal{C}^{\mathcal{T}}$. This set of paths is then rewritten into a ruleset as discussed in the next section.

5. RULE GENERATION

In this paper, we employ graph grammatical concepts to bridge the gap between global information that is available during planning and local information that is available to the cubes during reconfiguration. The centralized path planning results are rewritten into rules that can be checked locally for applicability. Contrary to rules only based on connectivity information, graph grammars offer fine-grained control over the applicability of rules and allow the encoding of additional information into the labels of the rules. Before we introduce our rule generation and execution approach, we define the graph grammatical terms used in this paper, taken from Klavins et al. [2006].

Definition 9. A *production rule* or simply a *rule* consists of two labeled graphs; a left-hand side g_l and a right-hand side g_r. It describes a transformation of a graph G_S, that is isomorphic to g_l, from G_S to g_r.

A graph grammar is a set of production rules that operate on a graph G_0. Therefore, we call the pair (G_0, Φ) a system, where G_0 is an initial labeled graph and Φ is a graph grammar. A rule $r \in \Phi$ can be applied to G_0 only when it is applicable:

Definition 10. A rule is *applicable* to G if there exists a subgraph G_S of G that is isomorphic to g_l. This is also denoted as $G_S \cong g_l$.

Once the applicability of a rule r to a subgraph G_S of G has been determined, r can be applied to G. The application of a rule r yields a new graph $G_i \xrightarrow{r} G_{i+1}$, where G_{i+1} results from G_i by replacing the subgraph G_S with g_r. Each step in the reconfiguration process yields a graph G_i that is part of a trajectory, i.e. a finite or infinite sequence $\sigma = \{G_i\}_{i=0}^{k}$ s.t. there exists a sequence of applicable rules $\{r_i\}_{i=0}^{k-1}$ where $r_i \in \Phi$ and $G_i \xrightarrow{r_i} G_{i+1}$. The set of all trajectories is denoted as $\mathcal{T}(G_0, \Phi)$ and the ith graph of $\sigma \in \mathcal{T}$ as G_i. Each graph G_i as part of a trajectory is called reachable by the system (G_0, Φ). A reachable graph can be temporary, such that some rule r in Φ is applicable to it, or stable (see Klavins et al. [2006]).

Definition 11. A graph G is *stable*, if no rule in Φ is applicable to it.

Stable graphs play an important role in this paper. In this section, we prove that the graph representing $\mathcal{C}^{\mathcal{T}}$ is the only reachable stable graph given a system (G_0, Φ). Here, G_0 is derived from $\mathcal{C}^{\mathcal{I}}$ and Φ is an automatically generated graph grammar. Furthermore, this section describes the structure of our rules, shows how we derive graphs from configurations of cubes, and presents the rule generation framework.

5.1 Rule Structure

For the purpose of self-reconfiguration, a production rule for our system uses the rule structure shown in Def. 9 and its two labeled graphs g_l and g_r are defined as follows:

$$g_l = f(\mathcal{N}_2(c_i, \mathcal{C}))$$
$$g_r = f(\mathcal{N}_2(c_i + m, \mathcal{C})),$$

f is given below but essentially maps from cubesets to graphs. $\mathcal{N}_2(c_i, \mathcal{C})$ is the immediate motion successor set of the current cube c_i in the configuration $\mathcal{C}$ and is given by $\mathcal{N}_2(c_i, \mathcal{C}) = \{c_j \in \mathcal{C} | c_i \in \mathcal{C} \wedge dist(c_i, c_j) \leq \sqrt{2}\}$. $\mathcal{N}_2(c_i, \mathcal{C})$ contains all cubes at a distance of one primitive motion from cube c_i. Both graphs, g_l and g_r, are derived from the sets $\mathcal{N}_2(c_i, \mathcal{C})$ and $\mathcal{N}_2(c_i + m, \mathcal{C})$ of c_i and its current motion m (given by the path planner) via the cubeset-to-graph mapping f.

Definition 12. The relationship between a cubeset $\mathcal{C}$ and a graph $G = (V, E, l_G)$ is given by the *cubeset-to-graph mapping f*, which is defined as $f = h \circ g$ such that $f(\mathcal{C}) = (V, E, l_G)$ with mappings g and h defined in Section 3. The inverse *graph-to-cubeset mapping* f^{-1} is given by $f^{-1} = g^{-1} \circ h^{-1}$ such that $f^{-1}(V, E, l_G) \ni \mathcal{C}$.

The application of a rule r to a subgraph G_S, i.e. $r(G_S \cong g_l) = g_r$, yields a new graph G'. The changes in the edge and label set described by $G = (V, E, l_G) \xrightarrow{r} (V, E', l'_G) = G'$ represent the motion in the configuration space, i.e. $\mathcal{C} = f^{-1}(G)$ and $\mathcal{C}' = f^{-1}(G')$, where c_i has been moved from $c_i \in \mathcal{C}$ to $c_i + m \in \mathcal{C}'$. Fig. 4 shows a graphical representation of $\mathcal{N}_2(c_i, \mathcal{C}) = f^{-1}(g_l)$ and $\mathcal{N}_2(c_i + m, \mathcal{C}) = f^{-1}(g_r)$ of some rule. The highlighted cube is the currently active cube c_i.

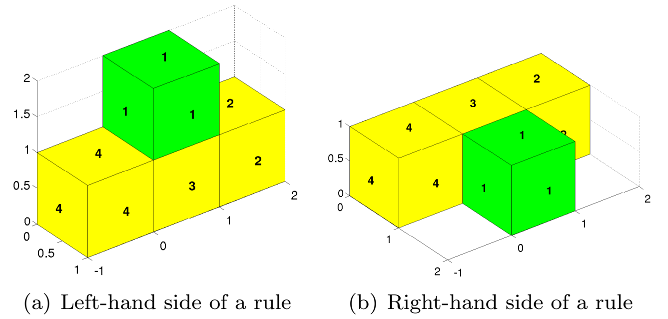

(a) Left-hand side of a rule (b) Right-hand side of a rule

Fig. 4. Visual representation of a rule that shows a convex motion of cube 1.

```
ID               : 130
gl_struct        : [1x1 struct]
gl_labels        : '114,130,1,25'
gr_struct        : [1x1 struct]
gr_labels        : '114,131,1,25'
update neighbors : []
```

Listing 1. Rule data structure

As part of g_l and g_r, each rule contains information about how the labels of the current node change through the application of the rule as well as optional label updates for the neighbors (see example in Listing 1). Since the labels of g_l and g_r in the rules we generate are essential in guaranteeing the properties of our reconfiguration approach, we will present a detailed description of their structure. Listing 1 shows that each label is composed of multiple, comma-separated data fields. These data fields include the *node ID*, the *rule ID*, a *flooding flag* indicating the start and the end of the flooding process, and a field storing the *latest finished path* (see fields *gl_labels* and *gr_labels* in Listing 1). The *node ID* and the *rule ID* are globally unique integers and ensure the uniqueness of each rule and the unambiguity of the whole reconfiguration. The *flooding* flag controls the start and end of the propagation process to update every node's knowledge about the latest finished path. The field *last path* concludes a label and stores the most recently finished path locally at every node. This field also controls the execution sequence of all individual paths, since the execution of path p_i depends on the conclusion of path p_{i-1}. The initial labeling of all nodes of the graph $G_0 = (V, E, l_G) = f(\mathcal{C}^{\mathcal{I}})$ and the label update mechanism through rules are designed so that only one rule is applicable to any cube $v_i \in V$ at any given time. Therefore, the reconfiguration is unambiguous and deterministic.

5.2 Rule Generation

The main contribution of this paper is the automatic generation of a graph grammar Φ that describes the unambiguous reconfiguration $\mathcal{C}^{\mathcal{I}} \xrightarrow{\Phi} \mathcal{C}^{\mathcal{T}}$. The path planning and the rule generation are interleaved, which means that once a path p_i ($i \in \{1..|P|\}$ where $|P| = |\mathcal{C}^{\mathcal{I}} \setminus \mathcal{O}_{init}| = |\mathcal{C}^{\mathcal{T}} \setminus \mathcal{O}_{init}|$) has been computed, the ruleset R_{p_i} that represents p_i is generated. R_{p_i} consists of $|p_i|$ motion rules, one flooding activation rule, and one propagation rule. More formally R_{p_i} is defined as $R_{p_i} = \{\{r_{m_i}\}_{i=1}^{|p_i|}, r_p, r_f\}$. The entire ruleset Φ is composed of all sub-rulesets R_{p_i}, i.e.

$\Phi = \{\{R_{p_i}\}_{i=1}^{|P|}\}$. The three types of generated rules are defined as follows:

Definition 13. A *motion rule* r_m changes the edge set and the label set of the graph $G = (V, E, l_G)$, specifically those edges whose end point is the current node v_i. Therefore, the application of a motion rule results in the motion of a cube c_i (represented by node $v_i \in G$) in the configuration space $\mathcal{C}$. More formally, r_m rewrites the graph $G = (V, E, l_G)$ the following way:

$$(V, E, l_G(v_i)) \xrightarrow{r_m} (V, E', l'_G(v_i))$$

The labels change from $l_G(v_i)$ to $l'_G(v_i)$ as follows:

$$l'_G(v_i) \rightarrow rule_id = l_G(v_i) \rightarrow rule_id + 1$$

Definition 14. A *flooding activation rule* r_f updates the *last path* field of the current node v_i and sets the *flooding* flag from 1 to 0, which activates the corresponding propagation rule. A flooding rule only affects the labels of the current node v_i and does change the edge set. Therefore, it does not result in a cube movement in the configuration space. More formally, r_f rewrites the graph $G = (V, E, l_G)$ the following way:

$$(V, E, l_G(v_i)) \xrightarrow{r_f} (V, E, l'_G(v_i))$$

The labels change from $l_G(v_i)$ to $l'_G(v_i)$ as follows:

$$l'_G(v_i) \rightarrow rule_id = l_G(v_i) \rightarrow rule_id + 1$$
$$l'_G(v_i) \rightarrow flooding = 0$$

Definition 15. A *propagation rule* r_p updates the current node v_i's labels by setting the *flooding* flag from 0 to 1 and incrementing the *last path* field of all its neighbors $v_j \in f(\mathcal{N}_2(c_i, \mathcal{C}))$. It also sets the *flooding* flag of its neighbors v_j to 0 so that the same rule r_p is applicable to them. This type of rule is a wildcard rule w.r.t. the node ID, i.e. it applies to every node independent of the node ID if all other label fields agree. A propagation rule does not change the edge set and therefore does not result in a cube movement in the configuration space. More formally, r_p rewrites the graph $G = (V, E, l_G)$ the following way:

$$(V, E, l_G(v_i, v_j)) \xrightarrow{r_p} (V, E, l'_G(v_i, v_j))$$

The labels change from $l_G(v_i, v_j)$ to $l'_G(v_i, v_j)$ as follows:

$$l'_G(v_i) \rightarrow rule_id = l_G(v_i) \rightarrow rule_id + 1$$
$$l'_G(v_i) \rightarrow path = l_G(v_i) \rightarrow path + 1$$
$$l'_G(v_i) \rightarrow flooding = 1$$
$$l'_G(v_j) \rightarrow flooding = 0$$

For each motion m_j in the path p_i, the neighborhood structure of two consecutive positions of the active cube is calculated and stored in a rule. Additionally, each rule stores the labels before and after the application of the rule (see example in Listing 1, fields *gl_labels* and *gr_labels*). More formally, for each motion m_j ($j \in \{1..|p_i|\}$ as defined in Def. 8) of path p_i, our algorithm generates a motion rule $r_{i,j}$ composed of g_l and g_r:

$$g_l = f(\mathcal{N}_2(c_i + (\sum_{k=1}^{j} m_k) - m_j, \mathcal{C})$$

$$g_r = f(\mathcal{N}_2(c_i + \sum_{k=1}^{j} m_k, \mathcal{C})$$

Here, c_i is the currently moved cube and the starting point of path p_i and $\mathcal{N}_2(c_i, \mathcal{C})$ is the immediate motion successor set as defined in Section 5.1. The labels of g_l are defined as follows:

$$l_G(g_{l_{i,j}}) = \begin{cases} l_G(g_{r_{i,j-1}}) & \text{if } j > 1 \\ l_G(g_{r_{i-1,length(p_i-1)}}) & \text{if } j = 1, i > 1 \\ l_{G,init} & \text{otherwise} \end{cases}$$

The labels of g_r are derived from the labels of g_l via the label update mechanism defined for motion rules, flooding rules, and propagation rules and can be summarized as follows.

$$l_G(g_{r_{i,j}}) = \begin{cases} l_G(g_{l_{i,j}}) \xrightarrow{r_m} l_G(g_{r_{i,j}}) & \text{for motion rules} \\ l_G(g_{l_{i,j}}) \xrightarrow{r_f} l_G(g_{r_{i,j}}) & \text{for flooding rules} \\ l_G(g_{l_{i,j}}) \xrightarrow{r_p} l_G(g_{r_{i,j}}) & \text{for propagation rules} \end{cases}$$

The labels are created with a strictly monotonically increasing global rule ID ensuring that each rule is globally unique and describes exactly one step in the complete reconfiguration sequence. Such a step is exemplified in Listing 1. The application of the shown rule with ID 130 changes the edge set of the immediate motion successor set of node 114 (specified by *gl_struct* and *gr_struct*) and updates its labels such that the next applicable rule is rule number 131 (see field *gl_labels and gr_labels*).

This process is repeated for every motion m_j of path p_i. After the end of the current path p_i is reached a flooding activation rule and a propagation rule are generated, resulting in a ruleset $R_{p_i} = \{\{r_{m_i}\}_{i=1}^{|p_i|}, r_p, r_f\}$. The rule generation process is repeated for every path p_i ($i \in \{1..|P|\}$) until the reconfiguration is completed, i.e. until the target configuration $\mathcal{C}^{\mathcal{T}}$ has been assembled. This means that the only reachable, stable graph as defined in Def. 11 is the graph representing the desired target configuration $\mathcal{C}^{\mathcal{T}}$.

Theorem 1. The graph $G = (V, E, l_G) = f(\mathcal{C}^{\mathcal{T}})$ representing the target configuration $\mathcal{C}^{\mathcal{T}}$ is the only reachable, stable graph to the ruleset Φ.

Proof 1. This proof is based on Theorem 1 in Rus and Vona [2001] and the definition and properties of a unit-modular self-reconfiguring system. Our system is composed of unit cubes, which can be assembled into arbitrarily shaped configurations. Thus our system satisfies property one. Property two states that in a configuration composed of unit modules, there always exists a module that can be relocated to any position on the surface S. In our system, S is defined as $S = \mathcal{N}_1(\mathcal{C}) = \{c_i | c_i \notin \mathcal{C} \wedge c_j \in \mathcal{C} \wedge dist(c_i, c_j) = 1\}$ and $\mathcal{R}$ is a subset of S, $\mathcal{R} \subset \mathcal{S}$. The movable set $\mathcal{M}$, on the other hand, is a subset of the boundary $\partial\mathcal{C}$ of $\mathcal{C}$, where $\partial\mathcal{C} = \{c_i | c_i \in \mathcal{C} \wedge |\mathcal{N}(c_i, \mathcal{C})| \leq 5\}$. $|\mathcal{M}| \geq 2$ according to Lemma 6 in Rus and Vona [2001] and only contains cubes $c_i \in \partial\mathcal{C}$. Therefore, our system fulfills property two of Theorem 1 as well. As a result, our system is self-reconfigurable and $\mathcal{C}^{\mathcal{T}}$ can be assembled incrementally from $\mathcal{C}^{\mathcal{I}}$. Therefore, every cube $c_i \in \mathcal{C}^{\mathcal{I}} \setminus \mathcal{O}_{init}$ will be moved to its target position $c_j \in \mathcal{C}^{\mathcal{T}}$. Since the current configuration $\mathcal{C}$ always remains connected (by construction of $\mathcal{M}$ and $\mathcal{R}$), i.e. $c(G) = c(f(\mathcal{C})) = 1$, a path always exists between c_i and c_j. The individual module paths are planned sequentially, which means that path p_{i+1} is planned after path p_i was planned and executed. This approach implicitly determines a unique reconfiguration sequence, i.e. the order in which all cubes are relocated. The outcome of the planning stage, i.e. the execution of

paths p_i for $i \in \{1, \dots, N\}$ with $N = |\mathcal{C}^{\mathcal{I}} \setminus \mathcal{O}_{init}|$, therefore, unambiguously yields $\mathcal{C}^{\mathcal{T}}$.

The rule and path generation are interleaved. After each path p_i has been planned, each motion m_j of p_i is rewritten into a rule $r_{i,j}$ with a globally unique rule number. These rule numbers are unique, strictly monotonically increasing, and are encoded in the labelsets of $r_{i,j}$. As a result, the applicability of rule $r_{i,j}$ depends on the successful execution of rule $r_{i,j-1}$. Therefore, the same sequence of reconfiguration steps is achieved as in the planning stage and the execution of the ruleset can only result in the target configuration $\mathcal{C}^{\mathcal{T}}$. Therefore, we can conclude that the only reachable, stable graph is $(V, E, l_G) = f(\mathcal{C}^{\mathcal{T}})$. □

5.3 Ruleset Execution

The goal of the ruleset execution is the reconfiguration of $\mathcal{C}^{\mathcal{I}}$ into $\mathcal{C}^{\mathcal{T}}$. In other words, given a system (G_0, Φ) we want to execute the assembly sequence $G_0 \xrightarrow{r_1} G_1 \xrightarrow{r_2} G_2 \xrightarrow{r_3} \dots \xrightarrow{r_n} G_{stable}$, where $G_0 = f(\mathcal{C}^{\mathcal{I}})$, $G_{stable} = f(\mathcal{C}^{\mathcal{T}})$, and n is the total number of rules. To accomplish this reconfiguration, every node $v_i \in \mathcal{G}$ periodically checks the ruleset for applicable rules $r \in \Phi$. If the graph represented by the current neighborhood $\mathcal{N}_2(c_i, \mathcal{C})$, i.e. $G_S = f(\mathcal{N}_2(c_i, \mathcal{C}))$ is isomorphic to the left-hand side g_l of some rule $r \in \Phi$, an applicable rule has been found and is applied to the current node v_i. Here, $c_i \in \mathcal{C}$ is the cube represented by node $v_i \in V$. The application of a rule r rewrites the subgraph G_S into g_r, i.e. $G_S \xrightarrow{r} g_r$. If the application of a rule changes the edge structure of G_S, which is the case only for motion rules, the cube c_i is moved in the configuration space. The execution of the last motion rule $r_{m_{i,|p_i|}}$ of a path p_i triggers a flooding activation rule r_{f_i}. This rule in turn triggers a propagation rule r_{p_i}. Through the repeated application of r_{p_i} to every node $v_i \in V$ every node's local state is updated about the completion of the latest path through directed flooding. This process is repeated until every path p_i is completed and no more rules in Φ are applicable to any node $v_i \in V$, i.e. until a stable graph is reached. An example of a reconfiguration sequence is shown in Fig. 7.

6. RESULTS

This section presents simulation results obtained in two experiments. We simulated the reconfiguration of overlapping configurations in the form of rectangular prisms (see Table 1) and the reconfiguration of overlapping random configurations (see Table 2). These configurations ranged in size from 100 to 500 modules. Our test system was equipped with an Intel Core i5-540M dual core processor and 4GB of DDR3 memory. Our simulator was implemented in Matlab 2010a running on Ubuntu 11.04.

The results of our simulations are shown in Table 1 and Table 2. In these tables, the field *Size* refers to the number of modules in the configuration, *Overlap* is the number of initially overlapping modules, *Steps* is the total number of motions of all modules to achieve the desired reconfiguration, *Rules* is the total number of rules in the ruleset, and *Runtime* is the time it took to generate the ruleset and complete the planning stage. As shown in Fig. 5 and Fig. 6 the size of the ruleset increases approximately linearly with the number of nodes, while the runtime of

Table 1. Reconfiguration planning results for overlapping box configurations

Size	Overlap [N]/[%]	Steps	Rules	Runtime [min]
100	30 / 30%	837	907	3.70
200	60 / 30%	1543	1683	16.65
300	90 / 30%	2426	2636	63.26
400	120 / 30%	3279	3559	135.64
500	150 / 30%	4275	4625	246.93

Table 2. Reconfiguration planning results for overlapping random configurations

Size	Overlap [N]/[%]	Steps	Rules	Runtime [min]
100	36 / 36%	352	416	2.25
200	114 / 57%	403	489	10.97
300	157 / 52.3%	893	1036	40.52
400	182 / 45.5%	1674	1890	120.84
500	231 / 46.2%	2327	2590	272.68

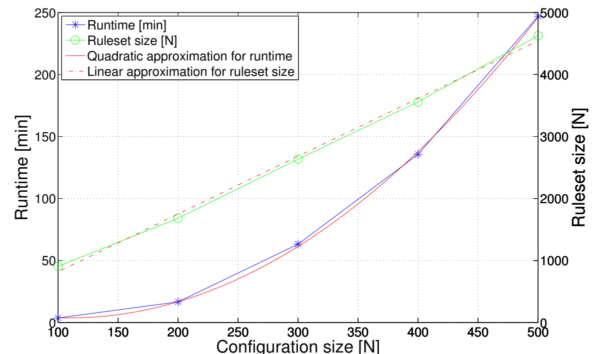

Fig. 5. Number of generated rules and required runtime for ruleset generation of box configurations

our algorithm increases approximately quadratically for the box and cubically for the random configurations. The runtime is primarily determined by the planning approach, which necessitates planning a path for every individual node. Our algorithm features a time complexity of $O(N^2)$ for the relocation of an individual cube and a total time complexity of $O(N^3)$ for the entire reconfiguration process. The experimental results shown in Fig. 6 confirm the expected time complexity of $O(N^3)$ while the results in Fig. 5 show only a quadratic dependency on the configuration size N. The reason for this behavior is that the Manhattan distance used as cost metric for A* is a significantly better heuristic for regular geometric shapes such as rectangular prisms. Therefore, the planning time for the reconfiguration of box configurations is lower compared to random reconfigurations even though the total path length is higher (as shown in Table 1 compared to Table 2).

7. CONCLUSIONS

In this paper, we have introduced an approach to automate reconfiguration planning and to automatically generate graph grammars. We have shown that our approach can reconfigure arbitrary configurations $\mathcal{C}^{\mathcal{I}}$ into any other arbitrary configuration $\mathcal{C}^{\mathcal{T}}$. We treat the reconfiguration

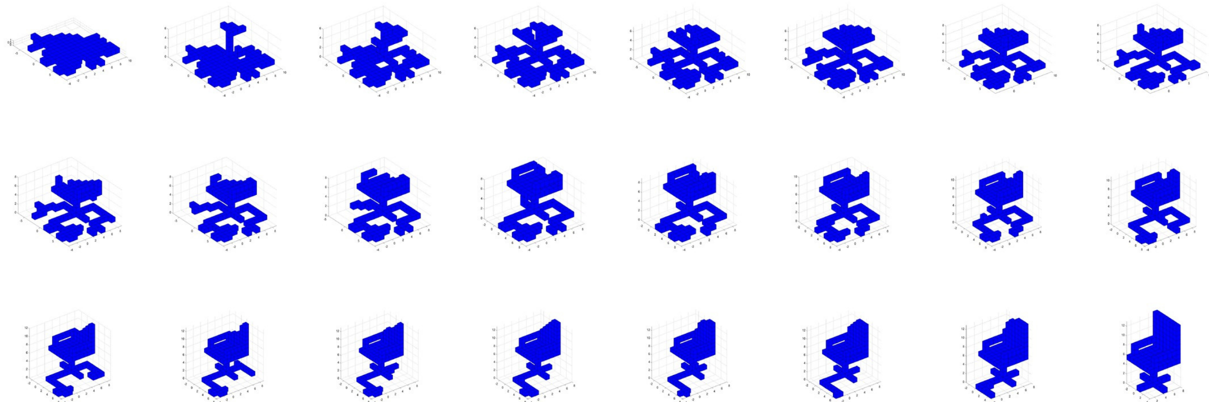

Fig. 7. Example of a reconfiguration sequence from a random two-dimensional configuration to a chair configuration.

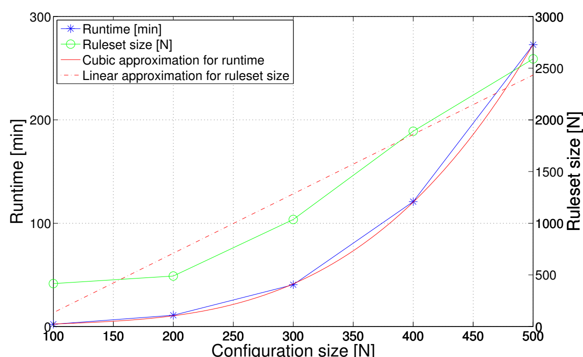

Fig. 6. Number of generated rules and required runtime for ruleset generation of random configurations

problem as a two-stage process containing a planning and execution stage. The centralized planning stage of our approach necessitates global knowledge of the configuration to generate the ruleset, while the decentralized execution stage works with local neighborhood information only. This is also the main advantage of our approach. While the generation of the ruleset features a time complexity of $O(N^3)$, the ruleset can be executed in a highly parallel fashion with each node checking simultaneously for applicable rules. Since the size of the ruleset grows approximately linearly in the configuration size N, this approach scales well.

REFERENCES

D. Brandt, D. J. Christensen, and H. H. Lund. Atron robots: Versatility from self-reconfigurable modules. In *In Proceedings of the IEEE International Conference on Mechatronics and Automation (ICMA)*, pages 2254–2260, Harbin, China, Aug. 2007.

David Brandt and Esben H. Ostergaard. Behaviour subdivision and generalization of rules in rule-based control of the atron self-reconfigurable robot, 2004.

Zack Butler, Keith Kotay, Daniela Rus, and Kohji Tomita. Generic decentralized control for lattice-based self-reconfigurable robots. *The International Journal of Robotics Research*, 23(9):919–937, 2004.

R. Fitch and Z. Butler. Scalable locomotion for large self-reconfiguring robots. In *Robotics and Automation, 2007 IEEE International Conference on*, pages 2248 –2253, April 2007.

R. Fitch, Z. Butler, and D. Rus. Reconfiguration planning for heterogeneous self-reconfiguring robots. In *Intelligent Robots and Systems, 2003. (IROS 2003). Proceedings. 2003 IEEE/RSJ International Conference on*, volume 3, pages 2460 – 2467, Oct. 2003.

Chris Jones and Maja J. Mataric. From local to global behavior in intelligent self-assembly. In *Proceedings of the 2003 IEEE International Conference on Robotics and Automation, ICRA 2003, September 14-19, 2003, Taipei, Taiwan*, pages 721–726. IEEE, 2003.

E. Klavins. Programmable self-assembly. *Control Systems, IEEE*, 27(4):43 –56, Aug. 2007.

E. Klavins, R. Ghrist, and D. Lipsky. A grammatical approach to self-organizing robotic systems. *Automatic Control, IEEE Transactions on*, 51 Issue: 6:949 – 962, 2006.

Daniela Rus and Marsette Vona. Crystalline robots: Self-reconfiguration with compressible unit modules. *Autonomous Robots*, 10(1):107–124, Jan. 2001.

Stuart J. Russell and Peter Norvig. *Artificial Intelligence: A Modern Approach*. Pearson Education, 2003. ISBN 0137903952.

Mark Yim, Wei-Min Shen, Behnam Salemi, Daniela Rus, Mark Moll, Hod Lipson, Eric Klavins, and Gregory S. Chirikjian. Modular self-reconfigurable robot systems – challenges and opportunities for the future. *IEEE Robotics and Autonomation Magazine*, March:43–53, 2007.